Solid State Communications 336 (2021) 114399

Contents lists available at ScienceDirect

Solid State Communications

journal homepage: www.elsevier.com/locate/ssc

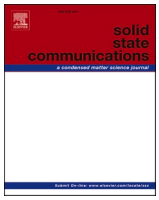

Investigation of structural, electronic and elastic properties of matlockite-type SrFI under high pressure: An Ab-initio study

Hülya Öztürk [a,*], Yılaydın Güzel [b], Cihan Kürkçü [c]

[a] Department of Physics, Kırşehir Ahi Evran University, Kırşehir, Turkey
[b] Institute of Science, Kırşehir Ahi Evran University, Kırşehir, Turkey
[c] Department of Electronics and Automation, Kırşehir Ahi Evran University, Kırşehir, Turkey

ARTICLE INFO

Communicated by

Keywords:
High pressure
Phase transformation
Electronic properties
Elastic constants

ABSTRACT

In this study, Matlockite (PbFCl) type SrFI compound with a two-dimensional layered structure has been studied using density functional theory (DFT) and generalized gradient approximation (GGA) under high hydrostatic pressure. Calculations were made using the Siesta Method. In ambient conditions, matlockite type structures crystallize in tetragonal structure with space group P_4/nmm. In nature, these structures are known as alkaline earth fluoro-halides. When gradually increasing pressures were applied to this structure, the phase transition was observed to the orthorhombic structure with space group Pmmn. In addition to these studies, some physical properties of SrFI, such as lattice parameters, bulk modulus, the derivative of the bulk modulus, and volume values were also calculated. On the other hand, total energy and enthalpy calculations were made to obtain the phase transition pressure values that are in good agreement with the experimental results. According to these calculations, phase transition pressure was predicted at about 44.8 GPa. Besides, how electronic and elastic properties of SrFI compound change with applied pressure were also examined. In the electronic structure calculations, about 5.09 eV band gap value was obtained for P4/nmm phase at 0 GPa pressure. Under increasing pressure, the 0.16 eV band gap value was calculated for the Pmmn phase of SrFI. According to these results, the stable phases obtained of the SrFI compound have semiconductor characters since the both phases have a conceivable band gap. In addition, elastic constants were calculated and two structures of SrFI were found to be mechanically stable.

1. Introduction

SrFI crystallizes in a PbFCl-type tetragonal structure with space group P_4/nmm under ambient conditions. It is also called a matlockite-type structure in the literature [1–15] and has 6 atoms in the unit cell. Atoms are located at the Wyckoff positions 2c (1/4, 1/4, z), z = 0.167333, 2c (1/4, 1/4, z), z = 0.6574, and 2a (3/4, 1/4, 0) for Sr, F, and I, respectively.

PbFCl-type structures attract a lot of attention because of their practical applications such as medical imaging [16,17] and sensor to measure the pressure in diamond anvil cells [18,19] in the literature. For example, Shen et al. [12] carried out high-pressure x-ray diffraction studies on BaFCl and BaFBr up to 50 GPa, SrFCl up to 42 GPa, and CaFCl up to 27 GPa using diamond anvil cell and synchrotron radiation. Liu et al. [1] have been performed some defects in the PbFCl crystal by using First-principles pseudopotential calculations. Besides, some theoretical studies have been done on the electronic properties of PbFCl type compounds [5,13]. Kanchana et al. [13] investigated the structural and electronic properties of SrFBr, SrFI, and CaFBr. They used the tight-binding linear muffin-tin orbital (TB-LMTO) method in their work. Hassan et al. [5] also studied the electronic properties of MFX (M = Sr, Ba, Pb; X = Cl, Br, I). They used the full-potential linearized augmented plane wave (FP-LAPW) method in their calculations. Reshak et al. [11] also analyzed the optical properties of SrFX (X = Cl, Br, I) using the FP-LAPW method. However, changes in the structure under high pressure have been missing in the literature. Besides, elastic calculations made on PbFCl-type structures are very few. To eliminate this deficiency, increased hydrostatic pressure was applied to the tetragonal structure of SrFI, and phase transition was achieved to the orthorhombic structure. Then, changes in the structural, electronic, and elastic properties of this structure were observed in the presence of pressure.

* Corresponding author.
E-mail address: hozturk@ahievran.edu.tr (H. Öztürk).

https://doi.org/10.1016/j.ssc.2021.114399
Received 28 January 2021; Received in revised form 21 May 2021; Accepted 24 May 2021
Available online 28 May 2021

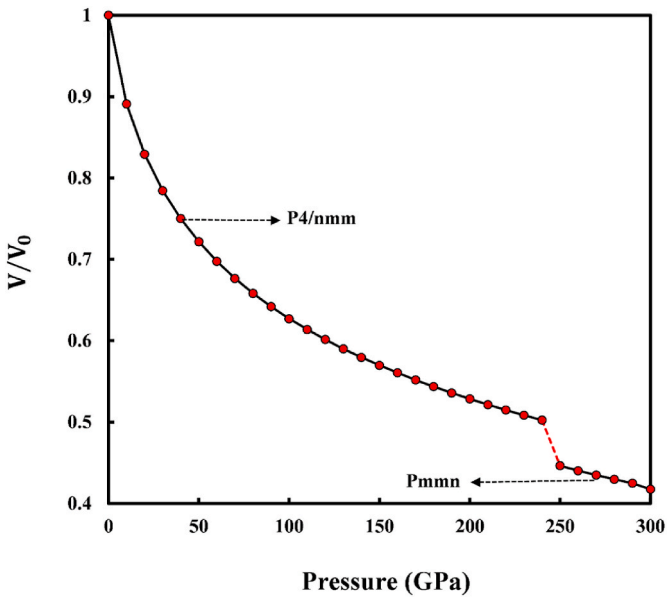

Fig. 1. Pressure-volume curve of the tetragonal type structure of SrFI.

Table 1
Transition pressure, lattice parameters and volume values for the obtained phases of SrFI.

Phases	P_t (GPa)	a (Å)	b (Å)	c (Å)	V(Å^3)	References
P_4/nmm	0	4.4469	4.4469	7.2801	143.96	This Study
		4.3050	4.3050	8.916	165.24	[6]
		4.2960	4.2960	8.888	164.03	[11]
		4.1730	4.1730	8.667	150.93	[13]
		4.2530	4.2530	8.8330	159.77	[38]
Pmmn	44.8	3.3250	3.6749	5.8469	71.44	This Study

2. Method

The structural, electronic, and elastic properties of SrFI are performed with the DFT method of the SIESTA [20] package using exchange-correlation functional of Generalized Gradient Approximation (GGA) with Perdew-Burke-Ernzerhof (PBE) [21]. SIESTA uses the standard norm-conserving pseudopotentials to get rid of the core electrons and allow for the expansion of a smooth (pseudo-) electron density on a uniform spatial grid. In this study, Troullier-Martins type pseudopotentials [22] were used for Sr, F, and I atoms. There are different basis set options in SIESTA. The double- ζ polarization (DZP) basis set which yields high-quality results for most of the systems was preferred in this study. As a result of the optimizations, the mesh cut-off value used in the calculations was found to be sufficient as 300 Ryd. Consisting of 72 atoms, the supercell structure of SrFI was modeled using periodic boundary condition with a 3 × 2 × 2. Brillouin zones (BZ) of SrFI for the obtained P_4/nmm and Pmmn phases were sampled with the 8 × 8 × 4 and 8 × 6 × 4 Monkhorst-Pack k-point mesh [23], respectively. Structural optimizations were performed via the conjugate gradient (CG) method until the residual forces acting on all atoms were smaller than 0.01 eV/Å. The gradually increased pressures of 10 GPa were applied to the P4/nmm phase of SrFI. The structures of SrFI at each pressure value were analyzed with the KPlot program [24]. As a result of the analysis, detailed information about lattice parameters, space groups, and atomic positions of the structures was obtained.

3. Results and discussions

3.1. Structural properties

Initially, before examining some of the physical properties of SrFI, such as structural, electronic, and elastic, the ground state crystal structure in the presence of 0 GPa pressure and 0 K temperature were determined as the tetragonal matlockite type structure belongs to space group P_4/nmm. After some optimizations applied to this structure, the lattice parameters of this tetragonal structure were obtained as a = b = 4.4469 Å and c = 7.2801 Å. When gradually increasing pressures were applied to this optimized structure, a sharply decrease in volume was observed at 250 GPa pressure. The curve of change in volume versus applied pressure is given in Fig. 1. As seen in this figure, there is a 10% collapse in volume at 250 GPa pressure. This collapse shows that there is a phase transition. Besides, the discontinuity in the volume is proof that the phase transition is of the first degree. Each pressure value applied to the system to reveal the presence of the phase transition was carefully analyzed and a phase transition to the orthorhombic structure with the space group Pmmn was obtained at 250 GPa. The lattice parameters of this orthorhombic structure were found as a = 3.3250 Å, b = 3.6749 Å, and c = 5.8469 Å. Also, in Table 1, transition pressure, lattice parameters and volume values for the obtained phases of SrFI are given with the other theoretical [6,11,13] and experimental [38] results.

The images of these phase structures obtained at 0 GPa and 250 GPa are given in Fig. 2.

In the next step, energy volume data were calculated for the predicted phases of the SrFI we worked on. The curve of change in total energy values as a function of the volume is shown in Fig. 3. The purpose of this calculation is to find out which of the phases obtained for SrFI is the most stable. As can be seen from Fig. 3, the lowest energy value was observed in the P_4/nmm phase of SrFI obtained at 0 GPa. Thus, the most stable structure of SrFI was predicted. While making this calculation, unit cells of SrFI were used. Besides, using the energy volume data, the value of the transition pressure from one phase to another can be calculated, and also calculate the bulk modulus by fitting to the third-order Birch-Murnaghan equation of states [25,26].

$$E = E_0 + \frac{9V_0B_0}{16}\left\{\left[\left(\frac{V_0}{V}\right)^{\frac{2}{3}} - 1\right]^3 B_0' + \left[\left(\frac{V_0}{V}\right)^{\frac{2}{3}} - 1\right]^2 \left[6 - 4\left(\frac{V_0}{V}\right)^{\frac{2}{3}}\right]\right\} \quad (1)$$

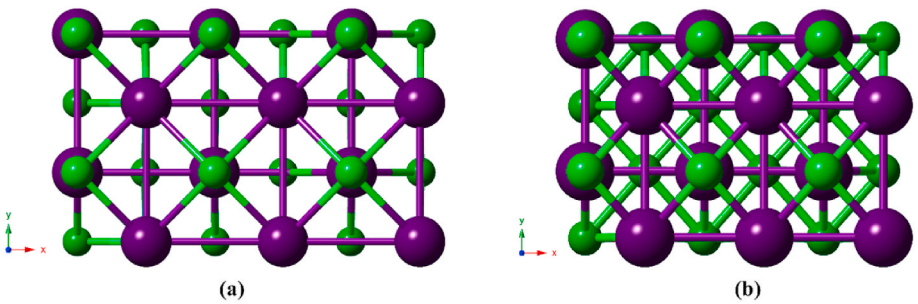

Fig. 2. Crystal structures of SrFI: (a) P_4/nmm at 0 GPa, (b) Pmmn at 250 GPa.

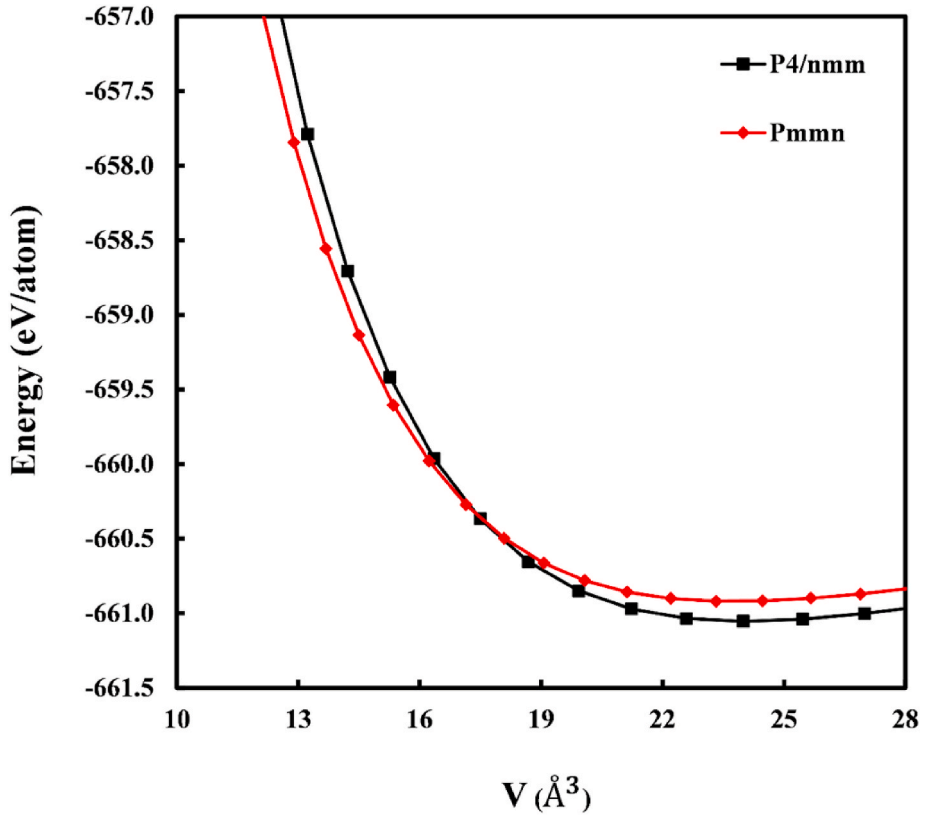

Fig. 3. Energy-volume curves for the obtained phases of SrFI.

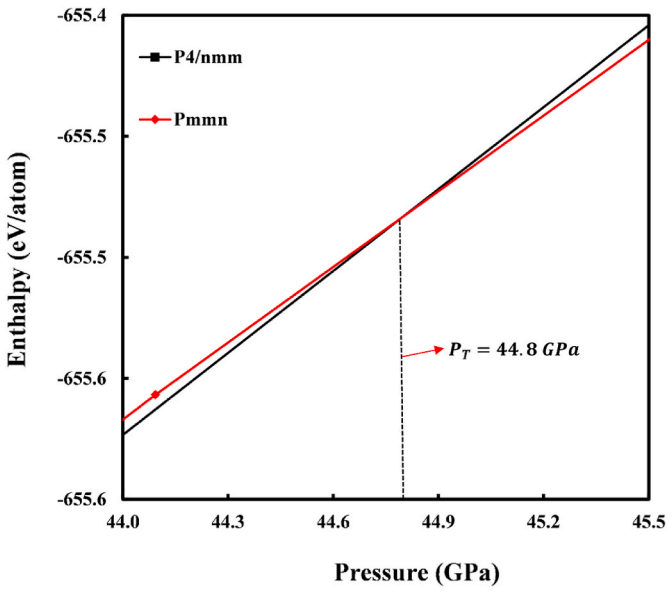

Fig. 4. Enthalpy curves for the obtained phases of SrFI as a function of pressure.

where E_0, V_0, and B_0 are energy, volume, and bulk modulus values at equilibrium, respectively. $B_0^{'}$ is the pressure derivative of the bulk modulus. Using Eq. (1), we can calculate the external pressure as follows:

$$P = -\left[\frac{\partial E}{\partial V}\right]_{T=0\ K} = \frac{3}{2}B_0\left[\left(\frac{V_0}{V}\right)^{7/3} - \left(\frac{V_0}{V}\right)^{5/3}\right] \times \left\{1 + \frac{3}{4}\left(B_0^{'} - 4\right)\left[\left(\frac{V_0}{V}\right)^{2/3} - 1\right]\right\} \quad (2)$$

In this study, the value of the transition pressure of SrFI from one phase to the other was obtained under high hydrostatic pressure by gradually increasing pressure. An ideal crystal structure consists of atoms/atom groups arranged by periodic boundary conditions and is not exactly perfect. There are some surface effects and defects in the crystal structure. However, a simulation system calculates by ignoring these effects and defects. Besides, the time scale in simulations is usually

Table 3
The Bulk modulus B (GPa), Shear modulus G (GPa), G/B and B/G ratios, Poisson's ratios (σ), and Young's modulus E (GPa) for the obtained phases of SrFI.

Phases	B	G	G/B	B/G	σ	E
P_4/nmm	32.54	21.01	0.65	1.55	0.234	51.87
Pmmn	420.45	75.71	0.18	5.55	0.415	214.275

Table 2
The elastic constants (GPa) for the obtained phases of SrFI.

Phases	C_{11}	C_{22}	C_{33}	C_{44}	C_{55}	C_{66}	C_{12}	C_{13}	C_{23}
P_4/nmm	80.87	–	30.65	23.42	–	26.69	19.05	23.37	–
Pmmn	439.28	567.42	578.20	8.77	165.99	273.90	201.81	372.86	319.16

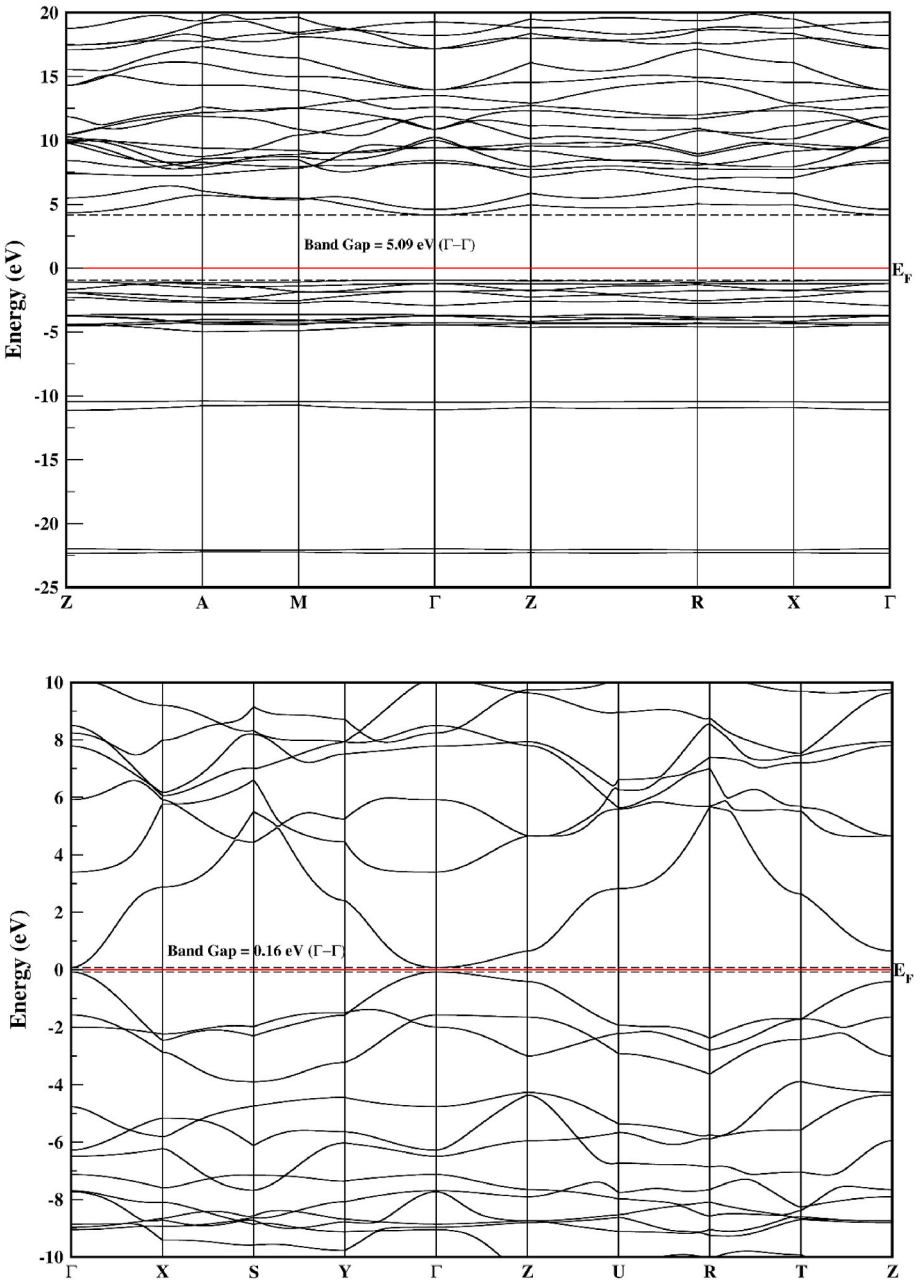

Fig. 5. The electronic band structures at 0 GPa (top), and 250 GPa (bottom) for SrFI.

shorter than that of experimental. In this short time scale, the structure may not have enough time to reconstruct or relax. Thus, frozen situations may occur in simulations [27]. Therefore, we compute enthalpy using thermodynamic calculations to predict the transition pressure values more compatible with the experimental results. We use energy-volume data when making this calculation, and Gibbs free energy (G) expression is given below to determine the most thermodynamically stable structure.

$$G = E_{tot} + PV - TS \quad (3)$$

where E_{tot}, P, V, T, and S are total energy, pressure, volume, temperature, and entropy, respectively. The structure of SrFI was studied at 0 K. Thus, in Eq. (3), the TS term is neglected and the G becomes equal to the enthalpy (H) as follows.

$$H = E_{tot} + PV \quad (4)$$

The enthalpy calculation as a function of pressure is given in Fig. 4. In this figure, the point where the two curves intersect gives the value of the transition pressure. For SrFI, this value has been predicted at about 44.8 GPa for $P_4/nmm \rightarrow Pmmn$.

3.2. Elastic properties

Elastic constants (C_{ij}) are important both theoretically and experimentally as they provide information about the hardness and stability of materials under applied strain and stress. Elastic constants were calculated for the tetragonal and orthorhombic structures of SrFI obtained under high pressure and are given in Table 2. Independent elastic constant numbers that provide information about the mechanical stability of the material are 6 (C_{11}, C_{12}, C_{13}, C_{33}, C_{44}, and C_{66}) for tetragonal structure [28] and 9 (C_{11}, C_{22}, C_{33}, C_{44}, C_{55}, C_{66}, C_{12}, C_{13}, and C_{23}) for orthorhombic structure [29,30]. Well known Born's stability criterion for the tetragonal structure is given below;

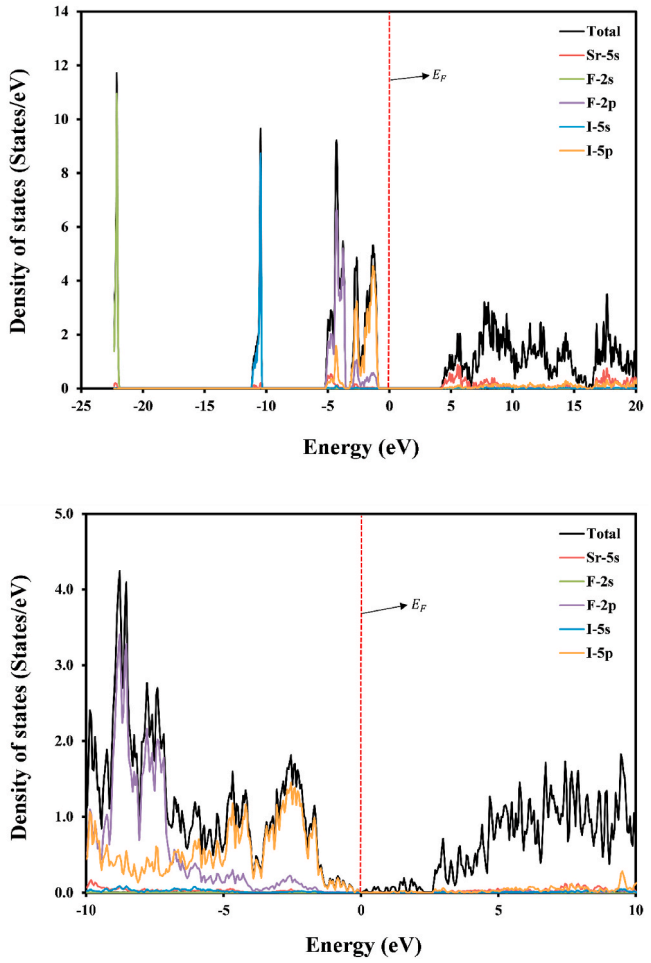

Fig. 6. The partial and total density of states at 0 GPa (top), and 250 GPa (bottom) for SrFI.

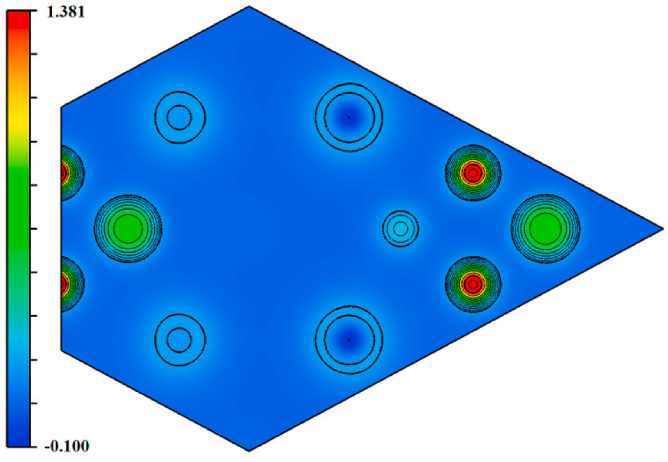

Fig. 7. The electronic charge density plot of the SrFI along the $[11\bar{2}]$ plane.

$$C_{11} > 0, C_{33} > 0, C_{44} > 0, C_{66} > 0, (C_{11} - C_{22}) > 0, (C_{11} + C_{33} - 2C_{13}) > 0, (2C_{11} + C_{33} + 2C_{12} + 4C_{13}) > 0 \quad (5)$$

Similarly, Born's stability criterion for the orthorhombic structure is as follows.

$$C_{11} > 0, \quad C_{22} > 0, \quad C_{33} > 0, \quad C_{44} > 0, \quad C_{55} > 0, \quad C_{66} > 0, \quad C_{11}C_{22}C_{33} + 2C_{12}C_{13}C_{23} - C_{11}C_{23}^2 - C_{22}C_{13}^2 - C_{33}C_{12}^2 > 0, \quad C_{11}C_{22} > C_{12}^2 \quad (6)$$

When the elastic constants in Table 2 are written into the above Born's stability criterion, it is seen that the SrFI phases are mechanically stable.

In Table 3, important parameters that provide information about the mechanical strength of the material obtained by using elastic constants are given. The first of these parameters is the bulk modulus (B), which is an indicator of the resistance to volume change under pressure. The resistance of the material changes directly with the increase in volume. When we look at Table 3, it is seen that the resistance of the Pmmn phase obtained under high pressure of SrFI is much higher. Therefore, the Pmmn phase is mechanically more stable [31]. The next parameter is the shear modulus (G), which is an indicator of resistance to shape change. According to Table 3, it is seen that the G value obtained for the Pmmn phase is higher. Thus, it is estimated that the Pmmn phase obtained for SrFI has a higher hardness. Besides, this result is in agreement with the bulk modulus.

Table 3 shows also the B/G ratio, which gives information about the brittleness and ductility of the material. As suggested by Pugh [32], if this value is below 1.75, the material is brittle, or if it is above 1.75, the material is ductile. Since the P_4/nmm phase has a value of 1.55, the material is brittle in this phase. However, when pressure of 250 GPa is applied to the material, the B/G ratio was estimated to be 5.55. Thus the Pmmn phase has a ductile feature.

In Table 3, the Poisson's ratio gives information about the bonding properties of the material. The Poisson's ratio also measures the stability of the crystal against shear. As higher the Poisson's ratio value gets the higher plasticity of the material [33]. In addition, as suggested in the literature, if the Poisson's ratio is around 0.1, the material has a covalent property. If it is around 0.25, the material has ionic properties [34,35]. The Poisson's ratio for the P_4/nmm phase of SrFI at 0 GPa pressure was estimated to be 0.234. Thus, the ionic character of SrFI is more dominant in this phase. For the Pmmn phase of SrFI under high pressure, the Poisson's ratio was obtained 0.415. Here, as in the first phase, the ionic character is more dominant. SrFI has ionically bound in both phases.

Young modulus (E) corresponding to the stiffness of the material is equal to the longitudinal stress divided by the strain. When the applied pressure increased, the stiffness of the material increased.

3.3. Electronic properties

The electronic properties for P_4/nmm and Pmmn phases of SrFI under 0 GPa pressure and high pressure were calculated along with the high symmetry directions. Fermi energy level was set to 0 eV while making calculations. Band structures are given in Fig. 5. As can be seen from the figure, there is a bandgap for both phases between the valence band and the conduction band. At 0 GPa pressure, the P_4/nmm phase has a bandgap of 5.09 eV [6,11,13]. When there is an increase in the pressure applied to the material, a decrease has been observed in this bandgap. The bandgap for the Pmmn phase was found to be 0.16 GPa. The maximum of the valence band and the minimum of the conduction band for both phases of SrFI are on the same symmetry point. Also, both materials have bandgaps. Thus, both phases of SrFI exhibit a direct bandgap semiconductor character.

In Fig. 6 a, the total and partial density of states were calculated for the phases of SrFI. For the P_4/nmm phase, as can be seen from Fig. 6 a, below the Fermi energy level, the largest contribution in the range (0) -

(- 4) eV comes from I-5s. In the range of (−4) - (- 5) eV, this contribution is due to F-2p. At approximately −10 eV and −22 eV, it is seen that the biggest contribution comes from I-5s and F-2s, respectively. The largest contribution above the Fermi energy level comes mostly from Sr-5s.

In Fig. 6 b, below the Fermi energy level, up to about −7 eV, the largest contribution comes from I-5p, while the largest contribution in the (−7) - (- 10) eV range comes from F-2p. Above the Fermi energy level, the biggest contribution comes from I-5p.

We also calculated the electronic charge density in order to have sufficient knowledge of the chemical nature of the compound. The electronic charge density is generally used to determine the type of chemical bonds linking the atoms [36,37]. Therefore, the two-dimensional electronic charge density distributions of SrFI under 0 GPa and high pressure are drawn using the Vesta program along the $(11\bar{2})$ plane and given in Fig. 7. As can be seen from this figure, the isoelectronic surfaces around all atoms are spherical in structure. Therefore, the bond type between atoms is ionic and this result is compatible with the type of bond obtained by the Poisson's ratio.

4. Conclusions

The structural, electronic, and elastic properties of SrFI under high pressure were investigated using DFT calculations. The phase transition from the tetragonal structure with space group P_4/nmm to an orthorhombic structure with space group Pmmn under pressure was predicted. The band structure calculations of the phases obtained showed that both phases have semiconductor character. The bandgap decreased from 5.09 eV to 0.16 eV with the increase in the pressure applied to the material. Also, it was found that both phases of SrFI were mechanically stable according to the calculated elastic constants. Information about the hardness of the material was obtained by using some important parameters predicted via elastic constants. It was also seen from the results that the hardness of the material increased when increasing pressure was applied to the SrFI.

Author statements

All authors contributed equally in this study.

Declaration of competing interest

We have no conflict of interest to declare.

References

[1] B. Liu, Z. Qi, C. Shi, First-principles study of the intrinsic defects in PbFCl, Phys. Rev. B 74 (2006) 174101.
[2] M. Canpolat, C. Kürkçü, Ç. Yamçıçıer, Z. Merdan, Structural and electronic properties of BiOF with two-dimensional layered structure under high pressure: ab initio study, Solid State Commun. 288 (2019) 33–37.
[3] F. Decremps, M. Fischer, A. Polian, J. Itie, M. Sieskind, Ionic layered PbFCl-type compounds under high pressure, Phys. Rev. B 59 (1999) 4011.
[4] G. Kalpana, B. Palanivel, I.S. Banu, M. Rajagopalan, Structural and electronic properties of alkaline-earth fluorohalides under pressure, Phys. Rev. B 56 (1997) 3532.
[5] F.E.H. Hassan, H. Akbarzadeh, S. Hashemifar, Theoretical study of structural and electronic properties of CaFI, J. Phys. Condens. Matter 16 (2004) 3329.
[6] F. El haj Hassan, H. Akbarzadeh, S. Hashemifar, A. Mokhtari, Structural and electronic properties of matlockite MFX (MSr, Ba, Pb; XCl, Br, I) compounds, J. Phys. Chem. Solid. 65 (2004) 1871–1878.
[7] A. Kushwaha, S. Akbudak, A. Yadav, Ş. Uğur, G. Uğur, Lattice dynamical and elastic properties of BaF X (X= Cl, Br and I): matlockite structure compounds, Int. J. Mod. Phys. B 33 (2019) 1950221.
[8] N. Subramanian, N.C. Shekar, P.C. Sahu, M. Yousuf, K.G. Rajan, Crystal structure of the high-pressure phase of BaFCl, Phys. Rev. B 58 (1998) R555.
[9] P. Labeguerie, F. Pascale, M. Merawa, C. Zicovich-Wilson, N. Makhouki, R. Dovesi, Phonon vibrational frequencies and elastic properties of solid SrFCl. An ab initio study, The European Physical Journal B-Condensed Matter and Complex Systems 43 (2005) 453–461.
[10] A.H. Reshak, Z. Charifi, H. Baaziz, First-principles study of the optical properties of PbFX (X= Cl, Br, I) compounds in its matlockite-type structure, The European Physical Journal B 60 (2007) 463–468.
[11] A.H. Reshak, Z. Charifi, H. Baaziz, Optical properties of the alkaline-earth fluorohalides matlockite-type structure SrFX (X= Cl, Br, I) compounds, Phys. B Condens. Matter 403 (2008) 711–716.
[12] Y. Shen, U. Englisch, L. Chudinovskikh, F. Porsch, R. Haberkorn, H. Beck, W. Holzapfel, A structural study on the PbFCl-type compounds MFCl (M= Ba, Sr and Ca) and BaFBr under high pressure, J. Phys. Condens. Matter 6 (1994) 3197.
[13] V. Kanchana, G. Vaitheeswaran, M. Rajagopalan, Electronic structure of ionic PbFCl-type compounds under pressure, J. Phys. Condens. Matter 15 (2003) 1677.
[14] M. Weil, F. Kubel, Matlockite-type PbFI, Acta Crystallogr. E: Structure Reports Online 57 (2001) i80–i81.
[15] Z.-L. Lv, H.-L. Cui, H. Wang, X.-H. Li, G.-F. Ji, Ab initio study of the structural, electronic, elastic and thermal conductivity properties of SrClF with pressure effects, Phil. Mag. 97 (2017) 743–758.
[16] T.K. Anh, W. Strek, C. Barthou, Energy transfer and dynamic luminescence of material containing rare earth ions used in X-ray medical imaging, J. Lumin. 72 (1997) 745–747.
[17] M. Secu, L. Matei, T. Serban, E. Apostol, G. Aldica, C. Silion, Preparation and optical properties of BaFCl: Eu2+ X-ray storage phosphor, Opt. Mater. 15 (2000) 115–122.
[18] Y. Shen, T. Gregorian, W. Holzapfel, Progress in pressure measurements with luminescence sensors, High Pres. Res. 7 (1991) 73–75.
[19] F. Decremps, M. Fischer, A. Polian, J.P. Itié, M. Sieskind, Ionic layered PbFCl-type compounds under high pressure, Phys. Rev. B 59 (1999) 4011–4022.
[20] P. Ordejón, E. Artacho, J.M. Soler, Self-consistent order-N density-functional calculations for very large systems, Phys. Rev. B 53 (1996) R10441.
[21] J.P. Perdew, K. Burke, M. Ernzerhof, Generalized gradient approximation made simple, Phys. Rev. Lett. 77 (1996) 3865.
[22] N. Troullier, J.L. Martins, Efficient pseudopotentials for plane-wave calculations, Phys. Rev. B 43 (1991) 1993–2006.
[23] H.J. Monkhorst, J.D. Pack, Special points for Brillouin-zone integrations, Phys. Rev. B 13 (1976) 5188.
[24] R. Hundt, J.C. Schön, A. Hannemann, M. Jansen, Determination of symmetries and idealized cell parameters for simulated structures, J. Appl. Crystallogr. 32 (1999) 413–416.
[25] F. Birch, Finite elastic strain of cubic crystals, Phys. Rev. 71 (1947) 809.
[26] F. Murnaghan, The compressibility of media under extreme pressures, Proc. Natl. Acad. Sci. U. S. A 30 (1944) 244.
[27] M. Durandurdu, Phase transition of ZrN under pressure, Phil. Mag. 99 (2019) 942–955.
[28] M. Özduran, A. Candan, S. Akbudak, A. Kushwaha, A. İyigör, Structural, elastic, electronic, and magnetic properties of Si-doped Co2MnGe full-Heusler type compounds, J. Alloys Compd. (2020) 155499.
[29] C. Kurkcu, S. Al, C. Yamcicier, Ab-initio study of structural, electronic, elastic, phonon properties, and phase transition path of sodium selenite, Chem. Phys. 539 (2020) 110934.
[30] S. Al, C. Kurkcu, C. Yamcicier, High pressure phase transitions and physical properties of Li2MgH4; implications for hydrogen storage, Int. J. Hydrogen Energy 45 (2020) 4720–4730.
[31] P. Li, J. Zhang, S. Ma, Y. Zhang, H. Jin, S. Mao, First-principles investigations on structural stability, elastic and electronic properties of Co7M6 (M= W, Mo, Nb) μ phases, Mol. Simulat. 45 (2019) 752–758.
[32] S. Pugh, XCII. Relations between the elastic moduli and the plastic properties of polycrystalline pure metals, The London, Edinburgh, and Dublin Philosophical Magazine and Journal of Science 45 (1954) 823–843.
[33] L. Liu, X. Wu, R. Wang, X. Nie, Y. He, X. Zou, First-principles investigations on structural and elastic properties of orthorhombic TiAl under pressure, Crystals 7 (2017) 111.
[34] V. Bannikov, I. Shein, A. Ivanovskii, Electronic structure, chemical bonding and elastic properties of the first thorium-containing nitride perovskite TaThN3, Phys. Status Solidi Rapid Res. Lett. 1 (2007) 89–91.
[35] S. Al, A. Iyigor, Structural, electronic, elastic and thermodynamic properties of hydrogen storage magnesium-based ternary hydrides, Chem. Phys. Lett. 743 (2020) 137184.
[36] A. Candan, A.K. Kushwaha, A first-principles study of the structural, electronic, optical, and vibrational properties for paramagnetic half-Heusler compound TiIrBi by GGA and GGA+ mBJ functional, Mater. Today Commun. 27 (2021) 102246.
[37] A. Gencer, A. Candan, A. Erkisi, Electronic nature, optical and mechanical properties ofM2Pt2O7 (M= Sc, Y and La) pyrochlores: A DFT study, Phys. B: Condens. Matter 607 (2021) 412862.
[38] H. Beck, A study on mixed halide compounds MFX (M= Ca, Sr, Eu, Ba; X= Cl, Br, I), J. Solid State Chem. 17 (1976) 275–282.